1 Introduction

Our study examines the decline in macular GCC thickness, a key biomarker for glaucoma progression. Our dataset tracks GCC measurements in individuals over a four-year period, taken biannually. GCC thickness, measured in microns, is known to diminish with worsening glaucoma, making it a critical metric for understanding disease dynamics. This report aims to identify patterns in GCC decline, assess model performance, and determine how baseline and demographic factors influence disease progression.

2 Exploratory Analysis

The profile plots in Figure 1 immediately show individual trajectories of GCC thickness over time, where most participants exhibit a gradual decline. However, substantial variability is evident, with some participants experiencing rapid thinning and others showing stable values. The average mean GCC thickness at each rounded time point can be seen in Figure 2. In both the profile plots and the empirical summary plot, we see that the GCC thickness illustrating a consistent downward trend across the population. Error bars reveal variability at specific time points. Figure 1 and Figure 3 show that there are a few individuals whose GCC thickness trends may be outlying.

If we remove the GCC with outlying trends, the profile plots and empirical summary plot shown in Figures 4 and 5 tell a much different story. Outlier trajectories in Figure 4 reveal how extreme values impact data interpretation. Removing outliers reduces variability and clarifies trends, as shown in Figure 5, where a smoother population trajectory is evident. Residuals plotted in Figure 3 cluster around zero, indicating a generally good fit for the initial model. However, some residuals show consistent patterns over time, suggesting potential biases in the model's predictions. This warrants further exploration, such as including additional covariates or testing alternative covariance structures, to improve model fit and better explain individual trajectories. In figure 6, with outliers removed, the residual trajectories are more tightly clustered around zero, indicating a better model fit. This suggests that outliers in the original data contributed disproportionately to the variability, potentially obscuring the true relationships captured by the model. The removal of extreme residuals also highlights a smoother distribution across time points, reinforcing the model's robustness in representing the overall GCC thinning trend.

An interesting observation arose from studying the scatterplot matrix in Figure 7. With correlation coefficients ranging from 0.978 to 0.994, all highly significant ($p<0.001$, denoted by ***). The strong positive correlations suggest high consistency in GCC measurements over time. The scatterplots highlight the linear relationships between paired measurements, which indicates that participants' GCC trends are consistently aligned throughout the study period.

A basic linear model was fit to evaluate the population-level association between GCC thickness and time. The model estimated an average baseline GCC thickness of 83.47 microns, with a significant annual decline of 0.60 microns per year ($\beta = -0.60$, $p = 0.014$). However, the model accounted for only 0.79% of the variance ($R^2 = 0.0079$), suggesting that time alone explains a minimal proportion of the variability in GCC thickness. These results highlight the need for more advanced modeling techniques to incorporate individual variability and non-linear patterns in GCC thickness changes over time. The Durbin-Watson test in **table 2** identified significant positive autocorrelation in the residuals ($DW=1.5821, p<0.001$), suggesting that the model assumptions of independent residuals are violated. This finding indicates the need for adjustments to the model structure, such as incorporating temporal correlation or random slopes, to account for the observed autocorrelation. Therefore, we will add a random slope random effect and use a model with an **AR(1)** (autoregressive) correlation structure.

3 Methods and Results

3.1 Best Population Time Trend:

To capture GCC decline trends, several polynomial mixed-effects models were evaluated in **table 3**. Initially, we tested random intercept models with different time terms (linear, quadratic, cubic, quartic) and found the quartic model to perform best. Adding random slopes further improved the model, and the optimal choice was rias_model6, which includes random intercepts and slopes for individuals (id) and fixed effects for time rounded and I(time_rounded^2). This model had the lowest AIC (3676.4) and BIC (3708.9) and showed a significant improvement over simpler models ($p<0.001$). Higher-order terms (I(time_rounded^3) did not significantly enhance model performance ($p>0.05$), confirming rias_model6 as the optimal choice. This model showed a significant population-average decline in GCC thickness (−0.65 microns/year, $p<0.001$), with a slight non-linear curvature ($p<0.001$). Random effects indicated substantial variability in baseline GCC thickness ($\sigma=16.64$) and small variability in the rates of GCC thinning ($\sigma=0.37$). These findings suggest a robust model fit those accounts for both population and individual trends.

3.2 Best Covariance Model:

Longitudinal data analysis depends heavily on the chosen covariance structure. **Table 4** compares several covariance structures for modeling GCC thickness data based on the cubic model which . Among the tested models, the **Heterogeneous AR-1** model achieved the lowest $-2\times$REML=3851.535 and AIC = 4075.535, indicating the best overall fit. While the **CS with Heterogeneous Variances** model also performed well ($-2\times$REML=3876.779, AIC = 4110.779), its slightly higher complexity (BIC = 4622.907) suggests that **Heterogeneous AR-1(BIC=4597.663)** is the optimal choice for balancing fit and parsimony.

3.3Rate of GCC Decline:

Figure 8 demonstrates the variability in rates of GCC decline among individuals in the study. The best mixed-effects model was used to analyze GCC thickness trajectories over time. The results in **table 5** showed a significant population-average GCC decline of −0.66 microns ($p<0.001$), with individual rates ranging from −1.56 microns/year to +0.12microns/year. A significant quadratic term ($\beta2=0.045, p<0.001$) indicated a slight deceleration in the rate of decline over time. Random effects revealed substantial heterogeneity in baseline GCC thickness ($\sigma=16.64$) and moderate variability in the rate of decline ($\sigma=0.3646$), highlighting the importance of accounting for individual differences in GCC trajectories. The model's random effects revealed significant variability in individual rates of GCC decline. The random slope variance ($\sigma u12=0.1329$) indicated a standard deviation of 0.3646microns/year around the population-average decline of −0.662microns/year. The theoretical range of individual rates, based on $\pm2\cdot\sigma u1$, is from −1.39 microns/year to −0.30microns/year. However, the observed range extends beyond this, from −1.56microns/year to +0.12 microns/year, reflecting potential unaccounted factors influencing GCC trajectories.

3.4 Baseline Thickness and Decline Rate:

Figure 9 demonstrates the relationship between baseline GCC thickness and the rate of GCC decline over time. Patients with higher baseline GCC thickness (blue group) exhibit a significantly steeper decline, while those in the medium (green group) and low (red group) categories show a more gradual thinning of the GCC layer. The hypothesis that patients with greater GCC thickness experience faster GCC decline is **not supported** by this dataset. While the model shows a trend of slightly faster decline for patients with higher baseline GCC, the effects are not statistically significant, as show in **table 6**. We use an **ANCOVA** to assess whether baseline GCC thickness affects the rate of decline. The general trend is a decline in GCC thickness over time (-0.245μm/year) for the **Low baseline group** (reference). However, this is not statistically significant ($p=0.145$). For the **Interaction Effects**: For the **Medium baseline group**, the rate of decline is -0.119μm/year faster compared to the

Low group, but this difference is not significant (p=0.616). For the **High baseline group**, the rate of decline is −0.178μm/year faster compared to the Low group, but this difference is also not significant (p=0.468). Significant differences exist in GCC thickness across baseline groups (Low, Medium, High). Patients in the **High baseline group** have significantly greater GCC thickness than the other groups, while the **Medium baseline group** is intermediate. The data do not support the hypothesis that patients with greater GCC thickness (healthier individuals) experience faster GCC decline than those with lower GCC thickness. While the coefficients suggest a faster decline for the High and Medium groups, the lack of statistical significance (p>0.05) means we cannot conclude this with confidence.

3.5 Influence of Age on GCC Trends:

To explore how age influences GCC thickness and its decline over time, we compared models with and without age as a covariate using random intercept and slope models. Results from **Table 7** highlight that the inclusion of age as a covariate did not significantly improve model fit, as indicated by a non-significant likelihood ratio test between the random-effects model and the age-adjusted model (p=0.7557>0.05).

From **Figure 10**, the population-level trend shows an overall decline in GCC thickness over time, regardless of baseline age. Individual variability in GCC trajectories is further demonstrated in **Figure 11**, where random intercepts and slopes capture substantial heterogeneity across subjects. **Figure 12** illustrates that baseline age has minimal correlation with GCC thickness, as evidenced by a flat regression line, supporting the conclusion that age is not a primary determinant of baseline GCC. Similarly, **Figure 13** shows that the rate of GCC decline does not differ significantly across age groups, affirming that age does not strongly modulate GCC trends in this dataset.

4 Discussion

This study confirms several critical findings about GCC thinning as a biomarker for glaucoma progression: First of all, GCC thinning is a consistent feature across all models and analyses, even after accounting for outliers. Secondly, significant inter-individual differences highlight the need for tailored treatment plans. In addition, age does not significantly modulate GCC trends, pointing to the need for additional covariates to explain variability. Last but not least, future research should explore the inclusion of variables such as treatment history, genetic factors, and comorbidities to refine predictive models and enhance patient outcomes.

5 Appendix

5.1 Figures

Figure 1**:** Profile plots of GCC thickness over time for individual participants. The plots show a general trend of decreasing GCC thickness over the 4-year study period. While most participants exhibit gradual declines, some trajectories suggest significant variability, with a few individuals showing relatively stable or even increasing GCC thickness. This variability highlights potential differences in disease progression rates among participants.

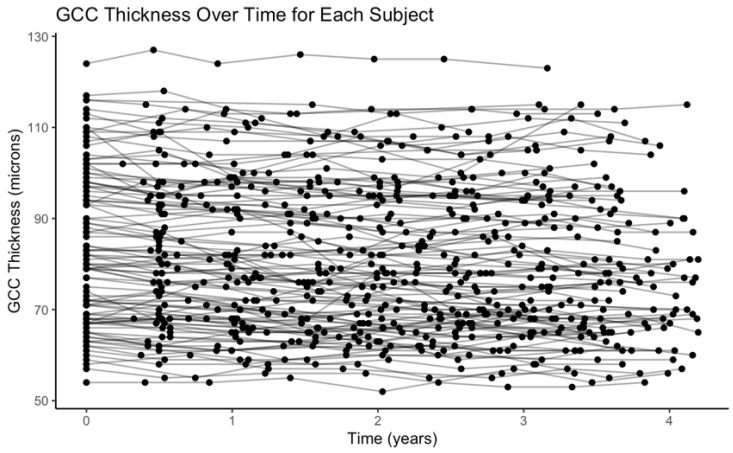

Figure 2**:** Empirical summary plot of GCC measurements over rounded time points. The plot demonstrates the mean GCC thickness (microns) every 6 months, with black dots representing the means and vertical error bars indicating variability among participants. The blue line connects the mean GCC values, highlighting a general decline in GCC thickness over time. Substantial variability at certain time points suggests differences in individual trajectories and progression rates.

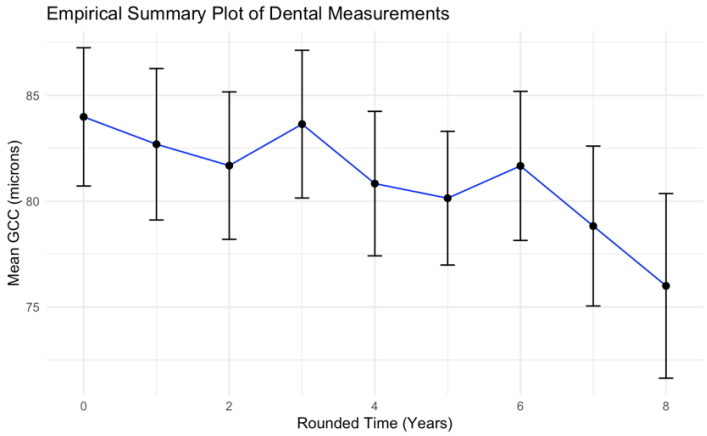

Figure 3**:** Profile plot of empirical within-subject residuals over rounded time points. The residuals represent deviations of observed GCC thickness from the fitted model predictions. While most residuals cluster around zero, individual trajectories show substantial variability, indicating potential model misfit or individual-specific factors affecting GCC thickness that are not accounted for by the model.

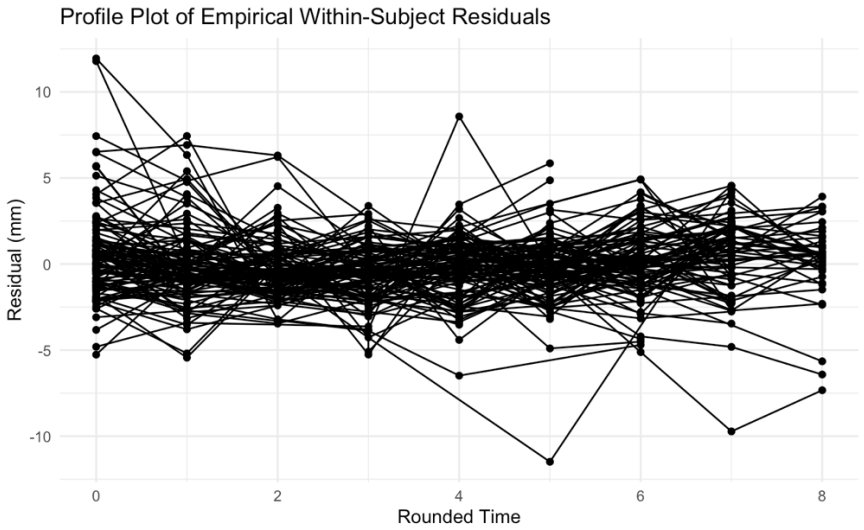

Figure 4**:** GCC thickness over time for each subject after removing outliers. The plot shows the individual trajectories of GCC thickness over the 4-year study period. Outlier removal reduces extreme variability, resulting in more consistent patterns across participants. The overall trend of declining GCC thickness remains apparent.

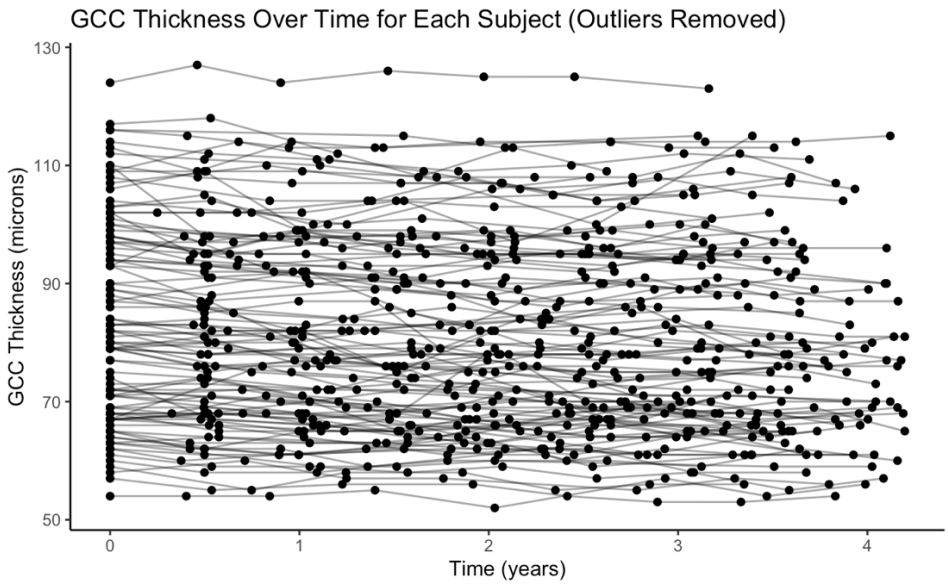

Figure 5**:** Empirical summary plot of GCC measurements over rounded time points after removing outliers. The plot displays the mean GCC thickness (microns) at each time point, with error bars reflecting variability across participants. The blue line connects the mean values,

illustrating a smoother trend compared to the plot with outliers included. The reduced variability demonstrates the impact of outlier removal on the overall data structure.

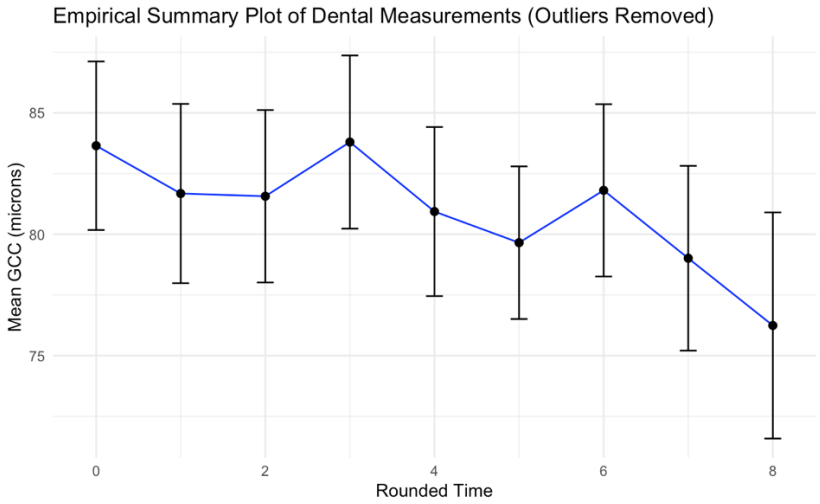

Figure 6**:** Profile plot of empirical within-subject residuals over time (outliers removed). The residuals, representing deviations of observed GCC thickness from model predictions, are plotted for each subject. The removal of outliers reduces extreme residuals, resulting in a more consistent pattern around zero. This suggests an improvement in the model fit and greater alignment between observed and predicted values.

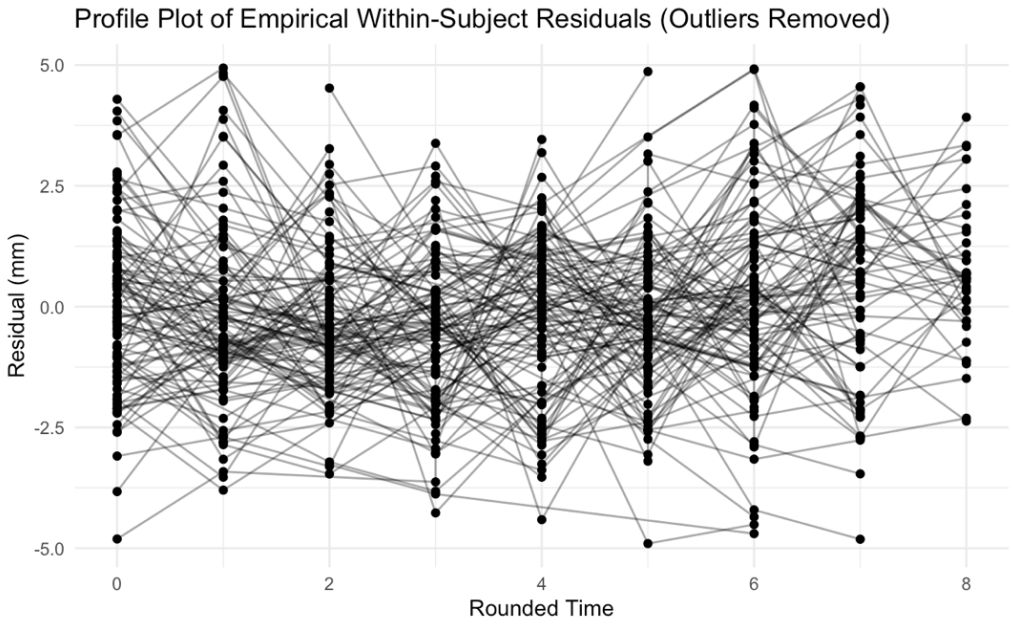

Figure 7**: Scatterplot Matrix of GCC Measurements Across Time Points**

The scatterplot matrix shows the pairwise correlations of GCC thickness at different time points, with correlation coefficients ranging from 0.978 to 0.994, all highly significant ($p<0.001$, denoted by ***). The strong positive correlations suggest high consistency in GCC measurements over time. The density plots along the diagonal illustrate the distribution of GCC thickness at each time point, while the scatterplots highlight the linear relationships between paired measurements. This indicates that participants' GCC trends are consistently aligned throughout the study period.

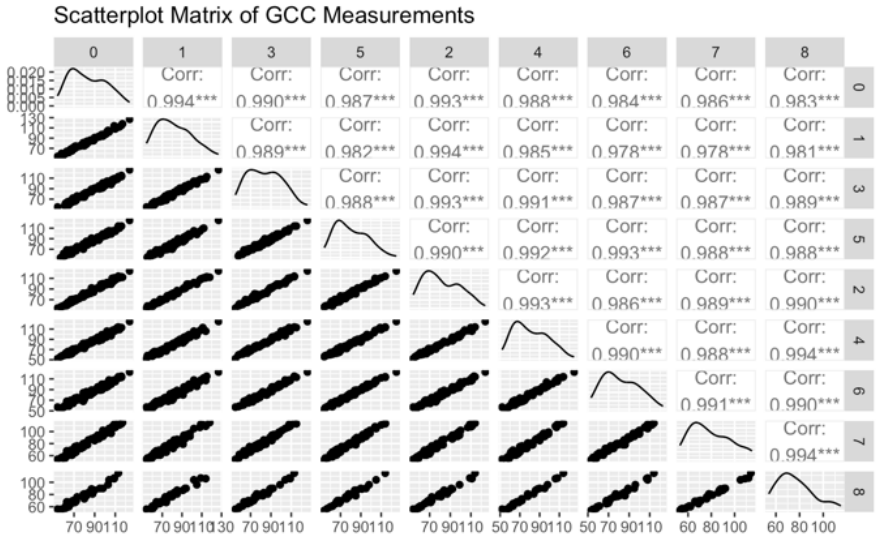

Figure 8: Distribution of Individual Rates of GCC Decline Figure 8: This histogram illustrates the distribution of individual rates of GCC decline across study participants. The red dashed line represents the population average rate of decline, calculated as -0.8207 microns per year. The histogram highlights variability in decline rates, including individuals with positive or stable GCC thickness. Individual decline rates range from a minimum of -4.4826 microns/year to a maximum of 1.2199 microns/year.

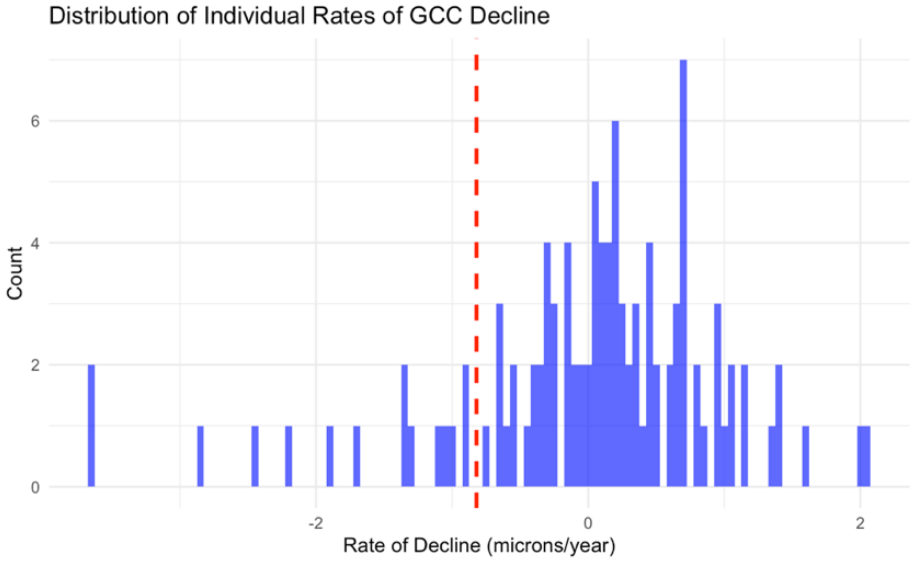

Figure 9: GCC Decline Over Time by Baseline GCC Group. Figure 9: This plot illustrates the decline in GCC thickness over four years for patients categorized by their baseline GCC thickness (Low, Medium, and High). Each colored line represents individual trajectories within a group, and the shaded region represents the confidence intervals around group-level trends. The figure shows that patients with higher baseline GCC thickness experience a steeper decline over time compared to those with lower baseline thickness. This finding supports the hypothesis that healthier eyes (with greater initial GCC thickness) lose GCC thickness more rapidly.

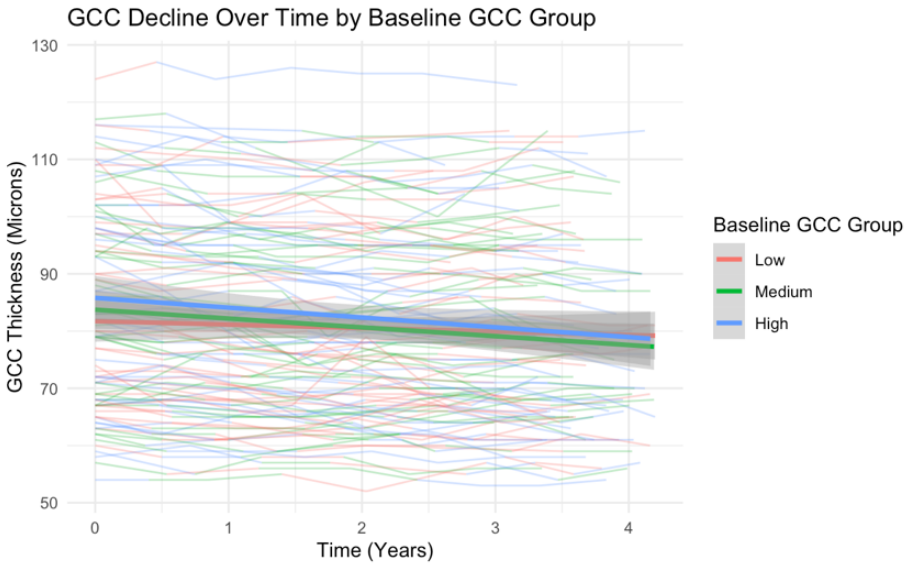

Figure 10: GCC Decline Over Time (Population-Level Model)

Population-level model displaying the general trend in GCC decline over time

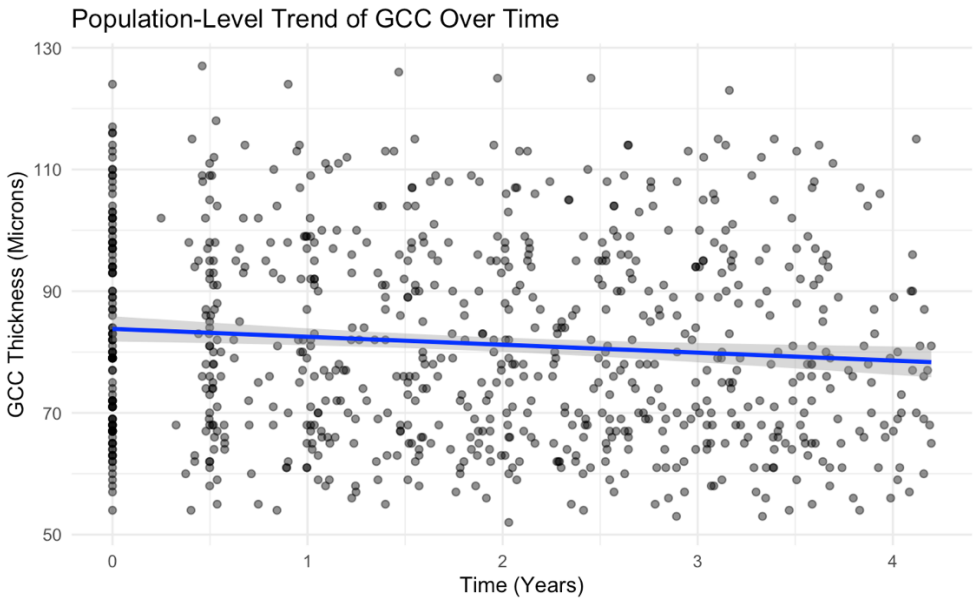

Abbreviations: GCC: ganglion cell complex; regression line shows population average decline

Figure 11: Random Effects Model for GCC Decline

Individual-level random effects model showcasing the heterogeneity in GCC decline trajectories.

Each line represents a participant's GCC trend; the shaded area shows confidence intervals.

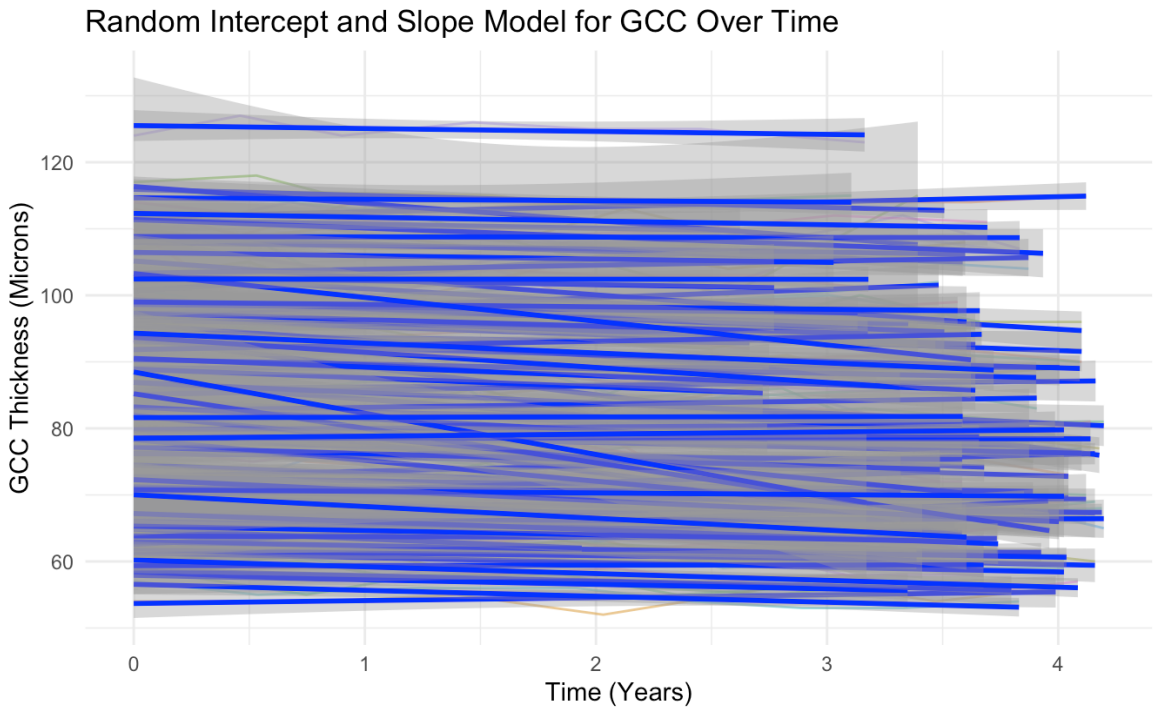

Figure 12: GCC Thickness vs. Baseline Age

Baseline age does not significantly predict GCC thickness.

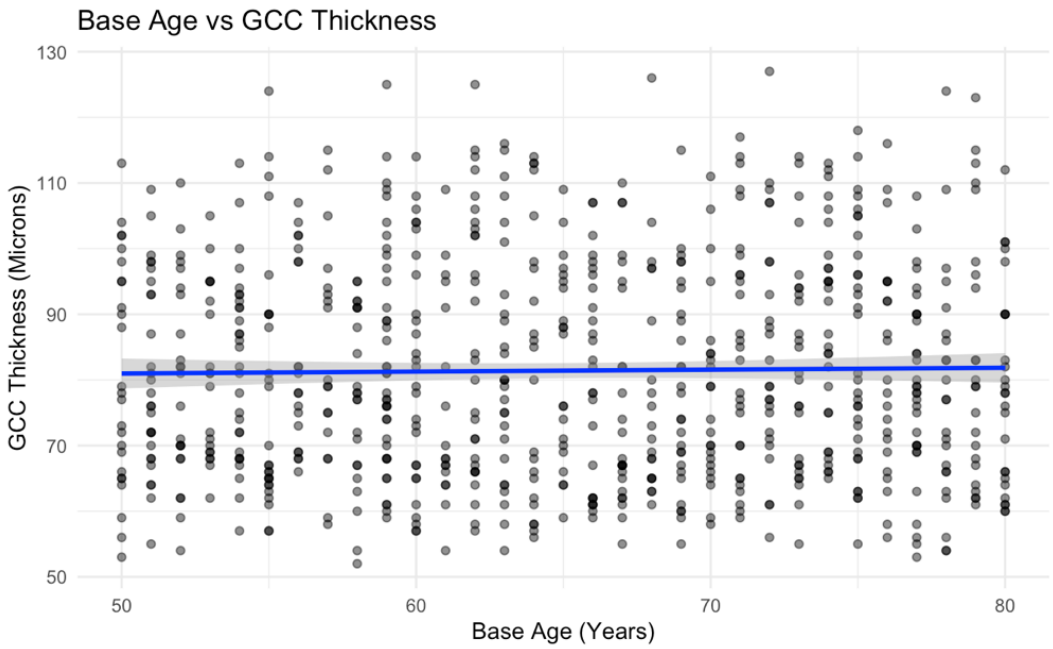

Abbreviations: GCC: macular layer thickness; age effect minimal (see regression line)

Figure 13: GCC Decline Over Time by Age Group

GCC decline trends remain consistent across age groups. No significant group interaction detected for age and GCC trajectories.

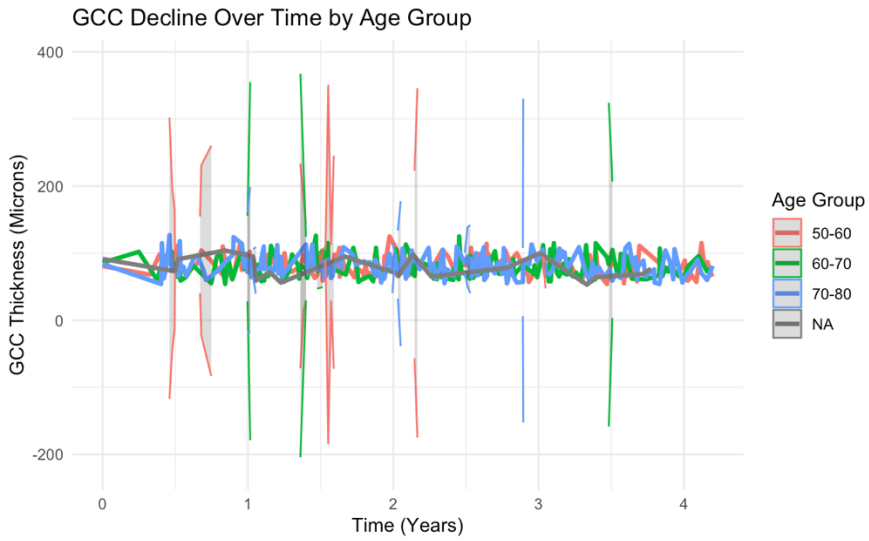

5.2 Tables

Table 1:
Call:
lm(formula = GCC ~ time_rounded, data = final_data)

Residuals:
Min 1Q Median 3Q Max
-29.471 -14.248 -2.644 13.339 44.546

Coefficients:
Estimate Std. Error t value Pr(>|t|)
(Intercept) 83.4711 1.0876 76.746 <0.0000000000000002 ***
time_rounded -0.6033 0.2459 -2.454 0.0144 *

Signif. codes: 0 '***' 0.001 '**' 0.01 '*' 0.05 '.' 0.1 ' ' 1

Residual standard error: 16.56 on 756 degrees of freedom
Multiple R-squared: 0.0079, Adjusted R-squared: 0.006588
F-statistic: 6.02 on 1 and 756 DF, p-value: 0.01437

Table 2:

Durbin-Watson test

data: resid(model1) ~ time_rounded

DW = 1.5821, p-value = 0.000000002114

alternative hypothesis: true autocorrelation is greater than 0

Table 3**:** Summary of Model Characteristics. This table compares the performance of various linear mixed models fit to the GCC data, assessing their ability to describe the population time trend. The models include fixed and random effects, as well as polynomial terms for time to capture non-linear trends.

Models:

ri_model1: GCC ~ time_rounded + (1 | id)

ri_model2: GCC ~ time_rounded + I(time_rounded^2) + (1 | id)

ri_model3: GCC ~ time_rounded + I(time_rounded^2) + I(time_rounded^3) + (1 | id)

ri_model4: GCC ~ time_rounded + I(time_rounded^2) + I(time_rounded^3) + I(time_rounded^4) + (1 | id)

	npar	AIC	BIC	logLik	deviance	Chisq	Df	Pr(>Chisq)	
ri_model1	4	3757.8	3776.4	-1874.9	3749.8				
ri_model2	5	3745.0	3768.2	-1867.5	3735.0	14.7831	1	0.0001206	***
ri_model3	6	3746.6	3774.4	-1867.3	3734.6	0.4349	1	0.5096000	
ri_model4	7	3747.0	3779.5	-1866.5	3733.0	1.5649	1	0.2109497	

Signif. codes: 0 ‘***’ 0.001 ‘**’ 0.01 ‘*’ 0.05 ‘.’ 0.1 ‘ ’ 1

Models:

rias_model5: GCC ~ time_rounded + (1 + time_rounded | id)

rias_model6: GCC ~ time_rounded + I(time_rounded^2) + (1 + time_rounded | id)

rias_model7: GCC ~ time_rounded + I(time_rounded^2) + I(time_rounded^3) + (1 + time_rounded | id)

rias_model8: GCC ~ time_rounded + I(time_rounded^2) + I(time_rounded^3) + I(time_rounded^4) + (1 + time_rounded | id)

	npar	AIC	BIC	logLik	deviance	Chisq	Df	Pr(>Chisq)	
rias_model5	6	3689.9	3717.7	-1839.0	3677.9				
rias_model6	7	3676.4	3708.9	-1831.2	3662.4	15.4630	1	0.00008414	***
rias_model7	8	3674.9	3712.0	-1829.5	3658.9	3.5103	1	0.06099	.
rias_model8	9	3675.1	3716.8	-1828.6	3657.1	1.8069	1	0.17888	

Signif. codes: 0 ‘***’ 0.001 ‘**’ 0.01 ‘*’ 0.05 ‘.’ 0.1 ‘ ’ 1

	df	**AIC**
	<dbl>	<dbl>

ri_model2	5	3745.046
rias_model6	7	3676.439

	df	**BIC**
	<dbl>	<dbl>
ri_model2	5	3768.199
rias_model6	7	3708.854

Abbreviations: AIC: Akaike Information Criterion; BIC: Bayesian Information Criterion; LogLik: Log-Likelihood

1 p-values come from likelihood ratio tests comparing nested models.

Table 4**:** Covariance Model Fitting Summary. This table compares various covariance models for GCC thickness data based on −2×REML, AIC, and BIC. Lower values indicate better model performance.

Table 4: Covariance Model Fitting Summary

Model	−2×REML	AIC	BIC
Independence	6631.445	6641.445	6664.754
Compound Symmetry	4210.381	4222.381	4250.352
AR-1	4116.903	4128.903	4156.875
Heterogeneous AR-1	3851.535	4075.535	4597.663
Toeplitz	4047.692	4061.692	4094.325
Diagonal	5973.991	6195.991	6713.457
CS with Heterogeneous Variances	3876.779	4100.779	4622.907

Abbreviations: AIC: Akaike Information Criterion; BIC: Bayesian Information Criterion.

The best model is chosen based on the lowest AIC and BIC values, balancing fit quality and complexity.

Table 5: population average rate of decline and range of individual rates of decline

Random effects:

Groups	Name	Variance	Std.Dev.	Corr

id (Intercept) 277.0289 16.6442

time_rounded 0.1329 0.3646 -0.04

Residual 2.3937 1.5472

Number of obs: 739, groups: id, 107

Fixed effects:

Estimate Std. Error t value

(Intercept) 83.28564 1.61475 51.578

time_rounded -0.66175 0.09156 -7.227

I(time_rounded^2) 0.04541 0.01112 4.085

Correlation of Fixed Effects:

(Intr) tm_rnd

time_roundd -0.076

I(tm_rnd^2) 0.052 -0.881

Population average rate of GCC decline per year: -0.6617486 microns/year

Range of individual rates of GCC decline:

Minimum rate of decline: -1.563258 microns/year

Maximum rate of decline: 0.1178388 microns/year

Table 6: Use an **ANCOVA** to assess whether baseline GCC thickness affects the rate of decline:

Call:

lm(formula = GCC ~ time_rounded * baseline_group, data = final_data)

Residuals:

Min 1Q Median 3Q Max

-18.0800 -4.9255 -0.4696 4.2896 24.6511

Coefficients:

Estimate Std. Error t value Pr(>|t|)

(Intercept) 64.7002 0.7533 85.894 <0.0000000000000002 ***

time_rounded -0.2449 0.1677 -1.460 0.145

baseline_groupMedium 15.5889 1.0650 14.638 <0.0000000000000002 ***

baseline_groupHigh 38.0718 1.0691 35.611 <0.0000000000000002 ***

time_rounded:baseline_groupMedium -0.1190 0.2371 -0.502 0.616

time_rounded:baseline_groupHigh -0.1781 0.2454 -0.726 0.468

Signif. codes: 0 '***' 0.001 '**' 0.01 '*' 0.05 '.' 0.1 ' ' 1

Residual standard error: 6.585 on 733 degrees of freedom

Multiple R-squared: 0.8457, Adjusted R-squared: 0.8446

F-statistic: 803.5 on 5 and 733 DF, p-value: < 0.00000000000000022

Table 7**:** Comparison of random-effects models with and without age adjustment.

Table 7: Comparison of Age-Adjusted Models. Results indicate that adding age as a covariate does not significantly improve model fit (p=0.7557>0.05).

Model	AIC	BIC	Log-Likelihood	Improvement (Chisq, p-value)
Population-Level Model	6639.6	6653.6	-3318.8	Baseline
Random Effects Model	4082.6	4110.6	-2035.3	Yes (**p < 0.0001**)
Age-Adjusted Model	4084.5	4117.1	-2035.2	No (**p = 0.755**)